Exploring the Tradeoff Between Energy Dissipation, Delay, and the Number of Backbones for Broadcasting in Wireless Sensor Networks Through Goal Programming[⋆]

Busra Gultekin[a,b], Derya Nurcan-Atceken[a,c], Aysegul Altin-Kayhan[a,*], Huseyin Ugur Yildiz[d], Bulent Tavli[e]

[a] *Department of Industrial Engineering, TOBB University of Economics and Technology, Ankara, 06560, Turkey*
[b] *Department of Industrial Engineering, TED University, Ankara, 06420, Turkey*
[c] *Department of Industrial Engineering, Ankara Science University, Ankara, 06570, Turkey*
[d] *Department of Electrical and Electronics Engineering, TED University, Ankara, 06420, Turkey*
[e] *Department of Electrical and Electronics Engineering, TOBB University of Economics and Technology, Ankara, 06560, Turkey*

Abstract

Broadcasting, which is an essential mode of operation in wireless sensor networks (WSNs), dissipates a non-negligible portion of the energy budget of a sensor node. Broadcasting is achieved by the dissemination of broadcast packets (originated at the BS) by a set of relay nodes, which constitute a backbone so that all sensor nodes receive broadcast packets. Utilization of multiple backbones is necessary to achieve balanced energy dissipation of sensor nodes in broadcasting. In this study, we propose two mixed integer programming (MIP) models (i.e., the flow-based model and the node-based model), which minimize the energy dissipation of the highest energy-consuming node for broadcasting by utilizing multiple backbones. Balanced energy minimization and delay minimization objectives are integrated through a goal programming (GP) framework built upon the foundation provided by the scalable node-based model. Performance evaluations based on the optimal solutions of our models reveal that maximum energy dissipation and delay in WSN broadcasting can be significantly reduced, simultaneously, by utilizing multiple backbones (e.g., with two backbones maximum energy dissipation and delay can be, concurrently, reduced by more than 2% and 22%, respectively, in comparison to the single backbone case, likewise, it is also possible to simultaneously reduce maximum energy dissipation and delay more than 8% and 13%, respectively, depending on the priorities assigned to the objectives). Nevertheless, employing more than two backbones does not provide any significant performance improvements.

Keywords: wireless sensor networks, broadcasting, mixed integer programming, goal programming, network lifetime, delay

1. Introduction

Wireless sensor networks (WSNs) are comprised of sensor nodes, which are, generally, small form factor devices with limited computation and communication capabilities, and one or more base stations (BSs), which is/are responsible for orchestrating the whole network. Commonly, a WSN is utilized to acquire information on the environment it is deployed over [1]. The first known use of WSNs was during the Vietnam conflict (i.e., operation Igloo White) [2]. WSN applications have proliferated rapidly, especially in the last two decades, which include military (e.g., battlefield surveillance, tracking of enemy forces), healthcare (e.g., continuous monitoring of high-risk cardiac/respiratory patients), smart homes/cities, transportation systems, and environmental applications (e.g., seismic movements and forest fire detection) [3].

Although unicasting of data from sensor nodes to the BS (i.e., convergecast) is, mostly, considered as the only traffic regime for WSNs, as the orchestrator of WSN operations, the BS also disseminates information to the sensor nodes via broadcasting, which is a relatively overlooked traffic regime in WSN literature. In fact, broadcasting plays a vital role in distributing control, management, and update information for WSNs [4]. Typically, broadcasting in a multi-hop network is done through a broadcast tree (i.e., a broadcast backbone) consisting of broadcast relay nodes and the source node. Each broadcast packet is transmitted by the source node and forwarded by the relay nodes in such a way that all the leaf nodes (i.e., passive listeners in a broadcast session) receive a broadcast packet from, at least, one member of the broadcast backbone [5, 6]. Two reference architectures showing sample broadcasting backbones in a 30-node WSN are presented in Figs. 1a and 1b. In these figures, the nodes colored red and blue are depicting leaf and relay sensor nodes, respectively, while the central black node is the base station, and the red line shows the constructed broadcast backbones.

Broadcasting is a non-negligible source of energy dissipation in a WSN, which becomes more demanding with increasing broadcast packet generation rate. Therefore, minimizing the sum of the energy spent in a WSN for broadcasting (i.e., the

[⋆] Busra Gultekin was supported by TÜBİTAK BİDEB 2210 Scholarship Programme.

[*] Corresponding Author

Email addresses: busra.gultekin@etu.edu.tr; busra.gultekin@tedu.edu.tr (Busra Gultekin), deryanurcan@etu.edu.tr; derya.nurcan@ankarabilim.edu.tr (Derya Nurcan-Atceken), aaltin@etu.edu.tr (Aysegul Altin-Kayhan), hugur.yildiz@tedu.edu.tr (Huseyin Ugur Yildiz), btavli@etu.edu.tr (Bulent Tavli)

minimum energy broadcast problem) is an important consideration to achieve overall energy efficiency in a WSN [7, 8, 9, 10]. However, minimizing the sum of the energy dissipation of all nodes does not necessarily result in the minimization of the maximum energy dissipating node's energy dissipation. Indeed, minimizing the aggregate energy dissipation of all nodes can lead to an unbalanced energy dissipation pattern (i.e., energy dissipation of certain nodes can become disproportionately higher than the others). In fact, this is similar to the WSN hotspot problem encountered in the convergecast traffic regime [11], which has a counterpart in the broadcast regime as well. Although there are alternative definitions of WSN lifetime, the time until the first node depletes its battery energy is, arguably, the most widely employed lifetime definition in the literature [12]. Hence, premature death of the higher energy-consuming nodes due to imbalanced energy dissipation patterns can lead to significant WSN lifetime reduction. To mitigate the unbalanced energy dissipation problem, minimizing the energy consumption of the maximum energy dissipating node (i.e., MinMax energy optimization) can be employed in WSN broadcasting, which results in the reduction of the excessively higher energy dissipation of any sensor node acting as a broadcast relay in comparison to the other relay nodes by creating optimal data flow patterns in a WSN [13].

The existing body of research on broadcasting in WSNs, mostly, considers a single broadcast backbone [5]. However, utilization of a single broadcast backbone results in considerably more energy dissipation of the relay nodes, constituting the backbone, than the leaf nodes in a WSN. Employing multiple broadcast backbones can, potentially, facilitate a more balanced energy dissipation strategy for broadcasting in comparison to a single broadcast backbone WSN scheme. Indeed, sensor nodes can be assigned varying roles in different broadcast backbones utilized in alternating time frames (e.g., a sensor node can act as a leaf node for a certain broadcast backbone while it acts as a relay node for another backbone), which enables the sharing of the energy cost of broadcast packet relaying among a wider set of nodes.

Minimizing delay in broadcasting is also an important consideration in WSNs [14, 15]. Broadcast traffic carrying time-sensitive information (e.g., network management packets) should be delivered to the entire network in a timely manner. In unicasting reducing the average path length results in lower delay. Likewise, reducing the broadcast backbone size leads to lower average broadcast packet delay [16, 17].

Energy efficiency in broadcasting can be achieved by utilizing the most energy-efficient backbones while not overburdening some nodes to create imbalanced energy dissipation patterns, however, such backbones do not, necessarily, include the shortest hop distance paths among the nodes. Delay minimization necessitates the average hop distance between the broadcast source and other nodes to be minimized [16, 17, 14, 15]. Therefore, minimizing delay and maximizing energy efficiency (i.e., minimizing the energy dissipation of the most energy-hungry node) are conflicting goals in WSN broadcasting (i.e., it is necessary to compromise the energy efficiency to design a low latency broadcast backbone and vice versa) [17, 6]. Using alternative backbones for broadcasting in WSNs adds flexibility in design for energy-efficient and delay-aware broadcasting. Goal programming (GP) is an effective approach for multi-objective optimization with conflicting objectives, which suits well in integrating the MinMax energy optimization and delay minimization objectives for the WSN broadcast problem allowing multiple backbones.

Nevertheless, systematic analysis of the tradeoff between energy efficiency and delay minimization for multiple backbone supporting broadcasting in WSNs under optimal operating conditions is an important research problem left unaddressed in the literature. To fill the aforementioned gap in the literature, in this study, we investigate and characterize the interplay between conflicting objectives of energy efficiency (within the MinMax energy optimization perspective) and delay minimization for broadcasting in WSNs over multiple backbones through a novel GP framework.

1.1. Major Contributions

The major contributions of this study are enumerated as follows:

1. We create two mixed integer programming (MIP) based optimization models (one has a flow-based packet flow formulation while the other model has a node-based packet flow formulation) to minimize the energy dissipation of the highest energy-consuming node for broadcasting over multiple backbones in WSNs. We also establish a delay-aware node-based MIP model to minimize the average delay in all backbones.
2. We construct a goal programming formulation built upon the scalable node-based MIP model, which minimizes the weighted relative deviations for the two conflicting objectives of MinMax energy optimization and delay minimization.
3. We integrate an empirically verified physical layer abstraction, which encompasses the channel model as well as the energy dissipation characteristics of a widely used sensor node platform in WSN literature [18], into our optimization framework.
4. The optimization models are solved to optimality for a vast parameter space to characterize the tradeoff between energy dissipation, delay, and number of backbones for broadcasting in WSNs.
5. Our results reveal that it is possible to decrease the maximum energy dissipation by increasing the number of backbones to two, yet, a further increase in the number of backbones does not bring any significant energy reduction.

The rest of the paper is organized as follows: Section 2 provides an overview of the related work on broadcasting in WSNs. Section 3 presents the network and energy models as well as the optimization framework for the broadcasting problem. Evaluations and insights based on the results obtained by the solutions of the optimization framework are given in Section 4. The conclusions of this study are drawn in Section 5.

2. Related Work

In this section, we present a concise overview of the literature, related to our study, on broadcasting in WSNs. A comprehensive literature review on WSN broadcasting is provided in [33]. A classification of broadcasting schemes, related to our work, according to objectives, utilized approaches, and the number of backbones is summarized in Table 1.

Much of the research on broadcasting is focused on the minimum energy broadcast problem to minimize the total energy consumed by the nodes during broadcasting [9, 19, 20, 8, 21, 7, 22, 16, 17, 6, 15, 23, 24, 4, 25]. In [20], the minimum energy broadcast problem is shown to be NP-complete. Wieselthier et al. [9, 19] introduce the broadcast incremental power (BIP) algorithm for constructing the minimum energy broadcast backbone for wireless networks. Several approaches are proposed to improve the BIP algorithm. Embedded wireless multicast advantage (EWMA) [8] and relative neighborhood graph broadcast oriented protocol (RBOP) [21] are two examples of such algorithms. In [4, 25], the minimum connected dominating set (MCDS) of nodes is utilized to generate energy-efficient broadcast backbones (i.e., minimizing the number of nodes in MCDS leads to the minimization of the total energy consumption).

There are several studies in the literature that investigate minimization of the energy dissipation of the maximum energy-consuming node (i.e., MinMax energy optimization) instead of minimizing the total energy consumption of the nodes in the network (as in the minimum energy broadcast problem) [26, 13, 27, 28, 29, 30]. In these studies, solving the MinMax energy optimization problem is shown to be equivalent to maximizing the WSN lifetime (i.e., the time until the first sensor dies – FSD) [28] under the condition that WSN nodes have equally distributed initial energies [13]. In [26, 28, 29, 30], the MinMax energy optimization problem is, explicitly, reformulated as the maximization of the FSD.

The issue of bounding delay in broadcasting has received considerable attention in the literature [16, 17, 6, 15, 31, 23, 32]. Reducing delay in broadcasting without considering energy efficiency is studied in [31, 32]. In [23], reducing delay in broadcasting is achieved by opportunistically selecting extra concurrent senders. Delay bounding constraints are incorporated into the minimum energy broadcast problem in [16, 17, 6]. Delay constraints enforce that the time required to propagate a broadcast packet to all nodes from the BS (i.e., the maximum delay observed in the network during broadcasting) is bounded by a certain threshold value, where the hop count metric is used for limiting broadcast latency. There are also several alternative definitions of delay in broadcasting such as the number of slots between sending a code from the sink node and reception of the code by leaf nodes [15], and the time between the first broadcast packet generated and the first given number of packets that are successfully delivered to the receiver within a certain time interval [31].

The research to date has tended to focus on the generation of a single rather than multiple backbones for energy-efficient and/or delay-aware broadcasting. To the best of our knowledge, a concurrent broadcast scheduling algorithm is proposed for lowering delay without relying on a predetermined broadcast backbone only in [32]. The two-step algorithm is designed to create a minimum-delay backbone structure and a receiver-based transmission schedule simultaneously. The multiplicity of backbones is obtained via dynamic role assignment to sensors. Indeed, the number of allowed backbones is not a controllable parameter in the model given in [32]. Therefore, the tradeoff between energy dissipation, delay, and the number of backbones is not explored systematically in [32]. On the other hand, the mathematical models in our study optimally decide on role assignments (e.g., relay or leaf node), number of backbones, and backbone structure. In our study, we investigate both delay and energy dissipation in WSN broadcasting unlike [32], which investigates only delay in broadcasting. Furthermore, we explore the impact of the number of backbones utilized, which has never been analyzed, systematically, under optimal operation conditions in the literature to the best of our knowledge.

The vast majority of the relevant literature considers algorithmic approaches (i.e., approaches apart from mathematical programming-based optimization). However, MIP-based optimization models, which are mostly cast as network flow problems, are developed to obtain energy-efficient broadcasting backbones in [22, 17, 24, 4, 29, 30]. Node-based [17, 4] or flow/link-based [22, 24, 29, 30] variables/constraints are employed in these models. Utilizing MIP models has the invaluable advantage that their optimal solutions provide theoretical best performances as target values for evaluating algorithmic solutions. While the solutions from different broadcast algorithms can be compared among themselves, the solution quality becomes hard to be judged without comparing to optimal solutions [24].

There are various studies in the literature, which utilize multi-objective optimization (MOO) models for investigating different goals in WSN broadcasting [16, 17, 6, 15, 31, 23]. In [15, 31, 23], algorithmic solutions are proposed to address MOO problems pertaining to WSN broadcasting. In [15], an algorithmic solution (i.e., proportion to duty cycle length based broadcast – PDLB) is presented for reducing delay in an energy-efficient manner. In [31], an adaptive multi-objective optimization model, which maximizes total transmission capacity and minimizes delay simultaneously, is proposed for vehicular ad hoc networks. In [23], an algorithmic solution based on adaptively selecting a set of concurrent senders is created for decreasing the broadcast delay while keeping the energy consumption at low levels. Total energy consumption and delay metrics are jointly minimized within MOO frameworks in [16, 17, 6], however, these studies do consider MinMax energy optimization. The ε-constraint method is utilized in [16, 17, 6], where the minimization of the total energy consumed by the nodes is kept as the single objective, while the minimization of delay is imposed as a constraint such that delay is bounded by some constant. However, limiting delay by a constant value is a serious drawback for obtaining all of the Pareto optimal solutions [34, 35]. To overcome the difficulties in generating the Pareto front when using the ε-constraint method, we propose an alternative technique for solving the MinMax energy

Table 1: Classification of studies on WSN broadcasting according to objectives, used approaches, and number of backbones.

Reference	Objective			Approach				# of Backbones	
	Total Energy Consumption	MinMax Energy	Delay	Algorithmic	MIP	Multi-Obj.	GP	Single	Multiple
[9, 19]	✓			✓				✓	
[20]	✓			✓				✓	
[8]	✓			✓				✓	
[21]	✓			✓				✓	
[7]	✓			✓				✓	
[22]	✓			✓	✓			✓	
[16]	✓		✓	✓		✓		✓	
[17]	✓		✓	✓	✓	✓		✓	
[6]	✓		✓	✓		✓		✓	
[15]	✓		✓	✓		✓		✓	
[23]	✓		✓	✓		✓		✓	
[24]	✓				✓			✓	
[4]	✓			✓	✓			✓	
[25]	✓			✓				✓	
[26]		✓		✓				✓	
[13]		✓		✓				✓	
[27]		✓		✓				✓	
[28]		✓		✓				✓	
[29]		✓			✓			✓	
[30]		✓		✓	✓			✓	
[31]			✓	✓		✓		✓	
[32]			✓	✓					✓
Our Work	✓	✓	✓		✓	✓	✓		✓

optimization and minimum delay MOO problem in an efficient way using the GP approach. Indeed, one of the main objectives of this study is to contribute to the literature by constructing a GP model for minimizing energy consumption as well as delay for WSN broadcasting.

GP is one of the most commonly used MOO approaches, which is a generalization of linear programming to address multiple conflicting objectives simultaneously [36, 37]. The motivation is to find a solution that minimizes the goal deviation, which is defined as a function of the difference between the desired value specified by the decision-maker and what can be achieved for each objective. The most commonly employed deviation functions are weighted sum, lexicographic, and MinMax [37]. Preferences of decision-makers among these objectives can be articulated via value functions or weights [36, 38]. It is shown in [39] that all MOO and GP approaches are actually special cases of the general weighted p-norm-based distance function. To this end, GP is a popular approach since it is relatively uncomplicated and easy to implement [36, 38, 40, 41]. However, applications of GP in WSNs are fairly limited [42, 41]), and we are not aware of any study that utilizes GP for analysis of broadcasting in WSNs. Hence, the creation of a GP-based MOO framework is one of our technique-wise contributions to the field as well.

In summary, to the best of our knowledge, there are no controlled studies in the literature on the joint optimization of the two conflicting objectives of MinMax energy optimization and delay minimization through GP in WSN broadcasting over multiple backbones, which can also be clearly observed by examining Table 1.

3. System Model

In this section, we present our system model organized under six subsections. In subsection 3.1, we introduce the network model we employ. In subsection 3.2, we outline our energy dissipation and path loss models. In subsections 3.3 and 3.4, we provide two MIP models for minimizing the energy dissipation of the maximum energy-consuming node with multiple backbones. The reason for creating two optimization models is two-fold. The first goal is to achieve independent confirmations of two independently constructed models for the optimal solution of exactly the same problem. The second goal is to benchmark the solutions times of flow-based and node-based models against each other so that we can pursue further analysis via the approach with lower solution times. In subsection 3.5, we present the optimization model, based on the node-based approach, with the objective of delay minimization. Subsection 3.6 elaborates on our novel GP model.

3.1. Network Model

We assume a static two-dimensional network topology consisting of a single base station (BS) and multiple sensor nodes. The deployment area is disk-shaped with radius 170 m and the BS is located at its center. Sensor nodes are deployed using a uniform distribution over the disk-shaped region. The network topology is modeled as a directed graph, $G = (V, A)$, where V is the set of all nodes including the BS (denoted by node-1) and A is the set of all arcs. The total number of sensor nodes (i.e., $|V|$) is varied between 20 and 70, where we use Mica2 motes as the sensor node platform. The operational time of the network is discretized into rounds of 60 seconds (i.e., $\mathcal{T}_{rnd} = 60$

Table 2: Energy Consumption Characteristics of the Mica2 mote platforms. $\mathcal{P}^c_{tx}(l)$ and $\mathcal{P}^o_{tx}(l)$ are the transmission power and the antenna output power (in mW) for the power level-l, respectively.

l	$\mathcal{P}^c_{tx}(l)$	$\mathcal{P}^o_{tx}(l)$	l	$\mathcal{P}^c_{tx}(l)$	$\mathcal{P}^o_{tx}(l)$
1 (l_{min})	25.8	0.0100	14	32.4	0.1995
2	26.4	0.0126	15	33.3	0.2512
3	27.0	0.0158	16	41.4	0.3162
4	27.1	0.0200	17	43.5	0.3981
5	27.3	0.0251	18	43.6	0.5012
6	27.8	0.0316	19	45.3	0.6310
7	27.9	0.0398	20	47.4	0.7943
8	28.5	0.0501	21	50.4	1.0000
9	29.1	0.0631	22	51.6	1.2589
10	29.7	0.0794	23	55.5	1.5849
11	30.3	0.1000	24	57.6	1.9953
12	31.2	0.1259	25	63.9	2.5119
13	31.8	0.1585	26 (l_{max})	76.2	3.1623

s). In each round, the BS broadcasts a packet of size $\lambda_P = 256$ Bytes to all nodes in the network periodically. We consider a 24-hour operation time for the WSN. Hence, the total number of broadcast packets generated is $M = 24 \times 60 = 1440$.

A node can either be a relay node that transmits the incoming packet or a leaf node that only receives but does not transmit it. The resulting backbone comprises the BS, relay nodes, and active links between them. Even a single change in sets of nodes or links leads to an alternative backbone, as we exemplify in Figs 1a and 1b. In this paper, we allow using multiple backbones for broadcasting to achieve both energy efficiency and delay minimization.

The overall energy consumption of each node is due to transmission, reception, and sleep mode. We assume that all nodes have omnidirectional antennas (i.e., all nodes within the communication range of a relay node can receive its transmissions). Therefore, the corresponding energy consumption of the transmitter is equal to the energy required to reach the farthest node by the wireless multicast advantage [9]. We provide further explanation about our energy model in Section 3.2. In addition, we adopt a log-normal shadowing path loss model to incorporate realistic communication characteristics in our optimization framework. Energy efficiency is achieved by employing MinMax energy optimization (i.e., minimizing the energy required by the most energy-consuming node). In fact, for a homogeneous WSN, lifetime maximization (i.e., according to the FSD metric) can, equivalently, be realized by MinMax energy optimization [13]. Furthermore, average total delay minimization can be garnered by minimizing the total number of hops from the BS to all nodes on the backbone [16, 17, 6], which is the definition we utilize in this study.

3.2. Energy Dissipation Model

We adopt the energy consumption model presented in [11] and employ the energy dissipation characteristics of the Mica2 sensor node platform [18]. Table 2 provides the energy consumption characteristics of the Mica2 motes for each discrete power level. Herein, for each power level $l \in L$, $\mathcal{P}^c_{tx}(l)$ is the power consumption of the transceiver, and $\mathcal{P}^o_{tx}(l)$ is the corresponding output antenna power. Moreover, the power consumption for reception (i.e., $\mathcal{P}^c_{rx}$) is denoted as 35.4 mW.

Each transmitter conveys a broadcast packet at a single time slot, which accounts for λ_P-Byte of a broadcast packet transmission, $\mathcal{T}_{tx}(\lambda_P)$ s, propagation delay, $\mathcal{T}_{rsp}$ =250 μs, and guard times, $2\times\mathcal{T}_{grd}$ =200 μs, applied both at the beginning and at the end of the active slot to avoid synchronization errors. Consequently, the slot time of each round is $\mathcal{T}_{slot} = 2\times\mathcal{T}_{grd}+\mathcal{T}_{tx}(\lambda_P)+\mathcal{T}_{rsp} = 107$ ms, where $\mathcal{T}_{tx}(\lambda_P)$ is computed as $\mathcal{T}_{tx}(\lambda_P) = 8 \times \lambda_P/\mathcal{R}_b$, where $\mathcal{R}_b = 19.2$ kbps is the data rate.

According to the log-normal shadowing path loss model, the path loss, $\overline{\mathcal{L}_{ij}}$ in dB, over the link-(i, j) is defined as

$$\overline{\mathcal{L}_{ij}} = \overline{\mathcal{L}_0} + 10 \times \eta \times \log_{10}\left(\frac{d_{ij}}{d_0}\right) + \overline{\mathcal{L}_\sigma}, \tag{1}$$

where d_{ij} is the link distance (in meters), $d_0 = 1$ m is the reference distance, $\overline{\mathcal{L}_0} = 55$ dB is the path loss at the reference distance, $\eta = 4$ is the path loss exponent, and $\overline{\mathcal{L}_\sigma}$ is a zero mean Gaussian random variable with standard deviation $\sigma = 4$ dB to capture the shadowing effect. The received signal power due to transmission at power level-l over the link-(i, j) is expressed as

$$\overline{\mathcal{P}^o_{rx,ij}(l)} = \overline{\mathcal{P}^o_{tx}(l)} - \overline{\mathcal{L}_{ij}}, \tag{2}$$

where the units of $\overline{\mathcal{P}^o_{rx,ij}(l)}$ and $\overline{\mathcal{P}^o_{tx}(l)}$ are dBm. Considering the noise power as $\overline{\mathcal{P}_n}$ =-115 dBm, the received Signal-to-Noise Ratio (SNR) at power level-l over the link-(i, j) is computed as (in dBm)

$$\overline{\phi_{ij}(l)} = \overline{\mathcal{P}^o_{rx,ij}(l)} - \overline{\mathcal{P}_n}. \tag{3}$$

Since Mica2 motes use non-coherent frequency- shift keying as the modulation scheme, on the average, a λ_P-Byte packet is successfully received with probability

$$\rho^s_{ij}(l) = \left(1 - 0.5\exp\left(\frac{-10^{0.1\times\overline{\phi_{ij}(l)}}}{1.28}\right)\right)^{8\times\lambda_P}. \tag{4}$$

To avoid retransmissions in case of packet failures, only the links with $\rho^s_{ij}(l) \geq 0.999$ are utilized (i.e., links with $\rho^s_{ij}(l) < 0.999$ are treated as unreliable and no broadcast packet transmissions are performed over such links).

Transmitting a λ_P-Byte broadcast packet using discrete power level-l over link-(i, j) dissipates $\mathcal{P}^c_{tx}(l)\mathcal{T}_{tx}(\lambda_P)$ energy. A node stays in reception mode after transmitting its packet. During reception, a node consumes $\mathcal{P}^c_{rx}(\mathcal{T}_{slot} - \mathcal{T}_{tx}(\lambda_P))$ energy. The total energy dissipated by a transmitter with packet processing cost (i.e., $\mathcal{E}_{PP} = 120$ μJ) is defined as

$$\mathcal{E}^l_{tx} = \mathcal{E}_{PP} + \left(\mathcal{P}^c_{tx}(l)\mathcal{T}_{tx}(\lambda_P) + \mathcal{P}^c_{rx}(\mathcal{T}_{slot} - \mathcal{T}_{tx}(\lambda_P))\right). \tag{5}$$

The total energy dissipation for receiving a λ_P-Bytes of a broadcast packet is expressed as

$$\mathcal{E}_{rx} = \mathcal{E}_{PP} + \mathcal{P}^c_{rx}\mathcal{T}_{slot}. \tag{6}$$

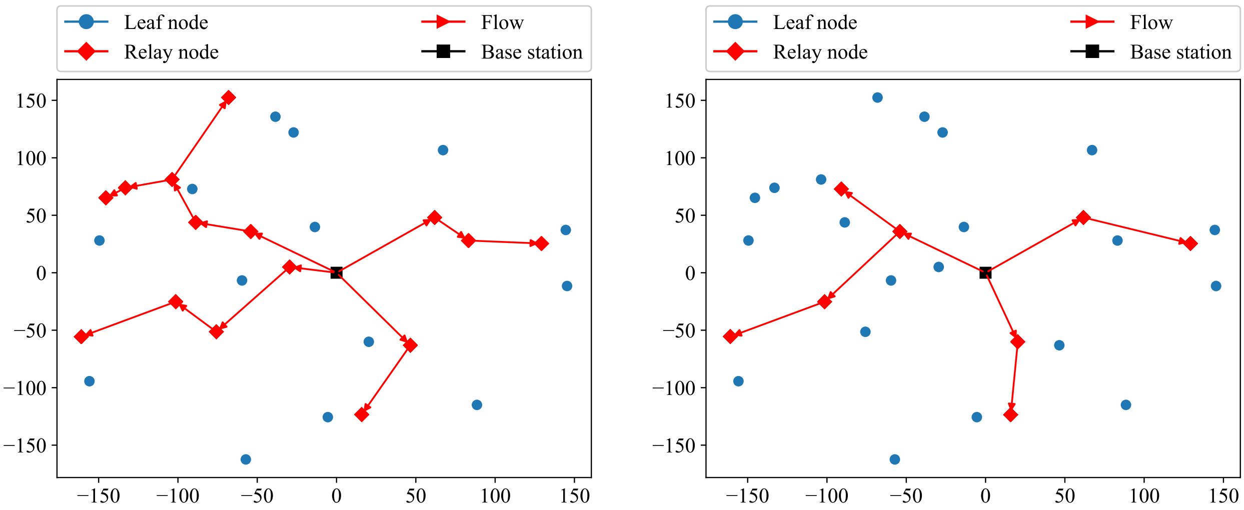

(a) 1st backbone structure

(b) 2nd backbone structure

Figure 1: Two example broadcast backbones on a 30-node sample network topology.

Table 3: Sets, parameters, and decision variables.

Sets	
V	All nodes including the BS ($V \in \{20, 30, \ldots, 70\}$)
W	All sensor nodes ($W = V \setminus \{BS\}$)
B	Backbones ($B \in \{1, \ldots, N_b\}$)
L	Power levels
Parameters	
N_b	The maximum number of backbones allowed ($N_b = \{1, 2, \ldots, 6\}$)
$\mathcal{P}_{slp}$	Power consumption in the sleep mode (3 μW)
$\mathcal{T}_{rnd}$	Duration of a round (60 s)
$\mathcal{T}_{slot}$	Active slot time (107 ms)
$\mathcal{E}^l_{tx}$	Energy dissipation of the transmitter at power level-l $\forall l \in L$
$\mathcal{E}_{rx}$	Energy dissipation of the receiver
M	The number of broadcast packets to be sent by the BS (1440)
a^j_{il}	1 if $j \in V$ can receive the packet sent by $i \in V \setminus \{j\}$ at power level $l \in L$, 0 otherwise
Variables	
x^b_{il}	1 if $i \in V$ transmits a packet at power level-$l \in L$ on backbone-$b \in B$, 0 otherwise
f^b_{ij}	1 if $i \in V$ transmits a packet to $j \in W \setminus \{i\}$ on backbone-$b \in B$, 0 otherwise
g^b_{ij}	1 if $j \in W$ receives its first packet from $i \in V \setminus \{j\}$ on backbone-$b \in B$, 0 otherwise
r^b_{il}	The total number of broadcast packets sent by $i \in V$ at power level-$l \in L$ on backbone-$b \in B$
m^b_{ij}	The total number of broadcast packets sent by $i \in V$ to $j \in W \setminus \{i\}$ on backbone-$b \in B$
u^b_i	The order of $i \in V$ receiving its first broadcast packet on backbone-$b \in B$
$\mathcal{T}^b_{bsy,i}$	The total busy time of $i \in V$ on backbone-$b \in B$
$\mathcal{E}_i$	The total amount of energy consumed by $i \in V$
$\mathcal{E}^{max}$	The amount of energy dissipated by the most energy-consuming node
s_b	The total number of broadcast packets distributed on backbone-$b \in B$

3.3. *The Flow-Based MIP (FB-MIP) Model for Minimizing the Maximum Energy Consumption*

In this subsection, we present the Flow-Based MIP model (FB-MIP) that can reconfigure WSN broadcast backbones. The aim is to minimize the energy dissipation of the highest energy-consuming node (MinMax energy optimization). The parameters, sets, and decision variables of FB-MIP are provided in Table 3. FB-MIP is presented in (7)–(45).

$$\text{Minimize} \quad \mathcal{E}^{max} \tag{7}$$

$$\text{s.t.} \quad \mathcal{T}^b_{bsy,i} = \mathcal{T}_{slot} \left(\sum_{l \in L} r^b_{il} + \sum_{j \in V \setminus \{i\}} m^b_{ji} \right), \quad \forall i \in W, b \in B \tag{8}$$

$$\mathcal{T}^b_{bsy,BS} = \mathcal{T}_{slot} \sum_{l \in L} r^b_{BS\,l}, \qquad \forall b \in B \tag{9}$$

$$\begin{aligned} \mathcal{E}_i = & \sum_{b \in B} \sum_{l \in L} r^b_{il} \mathcal{E}^l_{tx} + \mathcal{E}_{rx} \sum_{b \in B} \sum_{j \in V \setminus \{i\}} m^b_{ji} \\ & + \mathcal{P}_{slp} \left(\sum_{b \in B} s_b \mathcal{T}_{rnd} - \sum_{b \in B} \mathcal{T}^b_{bsy,i} \right), \qquad \forall i \in W \end{aligned} \tag{10}$$

$$\begin{aligned} \mathcal{E}_{BS} = & \sum_{b \in B} \sum_{l \in L} r^b_{BS\,l} \mathcal{E}^l_{tx} + \\ & + \mathcal{P}_{slp} \left(\sum_{b \in B} s_b \mathcal{T}_{rnd} - \sum_{b \in B} \mathcal{T}^b_{bsy,BS} \right) \end{aligned} \tag{11}$$

$$\mathcal{E}^{max} \geq \mathcal{E}_i, \qquad \forall i \in V \tag{12}$$

$$\sum_{b \in B} s_b = M \tag{13}$$

$$r^b_{il} \leq M x^b_{il}, \qquad \forall i \in V, l \in L, b \in B \tag{14}$$

$$r^b_{il} \leq s_b, \qquad \forall i \in V, l \in L, b \in B \tag{15}$$

$$r^b_{il} \geq s_b - M(1 - x^b_{il}), \qquad \forall i \in V, l \in L, b \in B \tag{16}$$

$$m^b_{ij} \leq M g^b_{ij}, \qquad \forall i \in V, j \in V \setminus \{i\}, b \in B \tag{17}$$

$$m^b_{ij} \leq s_b, \qquad \forall i \in V, j \in V \setminus \{i\}, b \in B \tag{18}$$

$$m^b_{ij} \geq s_b - M(1 - g^b_{ij}), \qquad \forall i \in V, j \in V \setminus \{i\}, b \in B \tag{19}$$

$$\sum_{l \in L} x^b_{il} \leq 1, \qquad \forall i \in V, b \in B \tag{20}$$

$$\sum_{l \in L} x^b_{il} \leq s_b, \qquad \forall i \in V, b \in B \tag{21}$$

$$s_b \leq M \sum_{l \in L} x^b_{BS\,l}, \qquad \forall b \in B \tag{22}$$

$$x^b_{il} a^j_{il} \leq f^b_{ij}, \qquad \forall i \in V, j \in W \setminus \{i\}, l \in L, b \in B \tag{23}$$

$$f^b_{ij} \leq \sum_{l \in L} x^b_{il} a^j_{il}, \qquad \forall i \in V, j \in W \setminus \{i\}, b \in B \tag{24}$$

$$x^b_{jl} \leq \sum_{i \in V \setminus \{j\}} f^b_{ij}, \qquad \forall j \in W, l \in L, b \in B \tag{25}$$

$$s_b \geq s_{b+1}, \qquad \forall b \in B, b \leq |B| \tag{26}$$

$$\sum_{i \in V \setminus \{j\}} f_{ij}^b \leq s_b, \qquad \forall j \in W, b \in B \tag{27}$$

$$M \sum_{i \in V \setminus \{j\}} f_{ij}^b \geq s_b, \qquad \forall j \in W, b \in B \tag{28}$$

$$u_i^b \leq u_j^b - 1 + (|V| - 1)(1 - g_{ij}^b), \quad \forall i \in V, j \in W \setminus \{i\}, b \in B \tag{29}$$

$$u_i^b \geq u_j^b - 1 - (|V| - 1)(1 - g_{ij}^b), \quad \forall i \in V, j \in W \setminus \{i\}, b \in B \tag{30}$$

$$u_i^b \leq u_k^b + (|V| - 1)(2 - g_{ij}^b - f_{kj}^b), \quad \forall i \in V, j \in W \setminus \{i\}, b \in B, k \in V \setminus \{i, j\} \tag{31}$$

$$g_{ij}^b \leq f_{ij}^b, \qquad \forall i \in V, j \in W \setminus \{i\}, b \in B \tag{32}$$

$$\sum_{i \in V \setminus \{j\}} g_{ij}^b = 1, \qquad \forall j \in W, b \in B \tag{33}$$

$$u_{BS}^b = 1, \qquad \forall b \in B \tag{34}$$

$$u_j^b \geq 2, \qquad \forall j \in W, b \in B \tag{35}$$

$$u_j^b \leq \sum_{i \in V} \sum_{l \in L} x_{il}^b + 1, \qquad \forall j \in W, b \in B \tag{36}$$

$$\mathcal{E}^{max} \geq 0 \tag{37}$$

$$f_{ij}^b,\ g_{ij}^b \in \{0, 1\}, \qquad \forall b \in B, i \in V, j \in V \tag{38}$$

$$\mathcal{E}_i \geq 0, \qquad \forall i \in V \tag{39}$$

$$\mathcal{T}_{bsy,i}^b \geq 0, \qquad \forall b \in B, i \in V \tag{40}$$

$$s_b \geq 0, \qquad \forall b \in B \tag{41}$$

$$r_{il}^b \geq 0, \qquad \forall b \in B, i \in V, l \in L \tag{42}$$

$$m_{ij}^b \geq 0, \qquad \forall b \in B, i \in V, j \in V \tag{43}$$

$$x_{il}^b \in \{0, 1\}, \qquad \forall b \in B, i \in V, l \in L \tag{44}$$

$$u_i^b \in \{0, 1\}, \qquad \forall b \in B, i \in V \tag{45}$$

The objective function (7) minimizes the energy consumption of the highest energy dissipating node in the network. We assume that all nodes except the BS are in sleep mode if they do not send or receive a broadcast packet. The total busy time of sensor node-i on the broadcast backbone-$b \in B$ (i.e., $\mathcal{T}_{bsy,i}^b$), which are the time slots required for both transmission and reception, is calculated in (8). The BS is busy only during transmission since it cannot be a receiver. Hence, the total busy time of the BS (i.e., $\mathcal{T}_{bsy,BS}^b$) is expressed in (9). The total energy dissipation of each node-i (i.e., $\mathcal{E}_i$) is equal to the sum of the energy consumed during transmission, reception, and sleep modes in all backbones as stated in (10). Note that $\mathcal{E}_{tx}^l$ and $\mathcal{E}_{rx}$ values are computed according to Equations (5) and (6), respectively. The total energy consumption of the BS during its busy time in all backbones (i.e., $\mathcal{E}_{BS}$) is defined in (11). The MinMax Energy objective is achieved with the help of Constraint (12). We include (13) to ensure that the BS delivers the required broadcast packets for a predetermined duration among all backbones (i.e., $\sum_{b \in B} s_b$). The motivation for fixing M a priori is to observe and evaluate the energy consumption behavior with different models for the same total traffic load of $M = 1440$ packets.

Constraints (14)–(16) equate the number of broadcast packets transmitted by a relay node in any backbone to the number of packets distributed in that backbone. On the other hand, (17)–(19) ensure that the number of packets received in any backbone by any leaf node is equal to the number of packets the BS injects in that backbone. Constraint (20) implies that not every node has to be a transmitter. If that is the case, each node must convey broadcast packets using a single power level in each backbone. Moreover, (21) and (22) together prevent role assignment to nodes in an unused backbone. Constraints (23) and (24) define the available transmission range, and hence the set of single-hop connections from each sensor based on its power level. In these constraints, we ensure that the relay node transmits broadcast packets to all nodes within its communication range but not beyond. Furthermore, if no other node transmits a packet to a node $j \in W$, then the node-j cannot be a relay node in that backbone as (25) states. Given N_b as the maximum number of useable backbones, we guarantee that utilized backbones are numbered consecutively in (26). Constraints (27) and (28) define the lower and upper bounds on the number of packets to be distributed on each backbone used as 1 and M, respectively.

The Miller-Tucker-Zemlin (MTZ) sub-tour elimination constraints adapted for broadcasting are given by (29) and (30). In our scheme, a sensor can get the broadcast packet from different sensors. Herein, for each backbone, (31) and (32) determine the first relay node from which a sensor receives a packet, whereas (33) ensures that this first node is unique for each sensor. Moreover, (34) initializes the BS as the first node in any backbone, and all other sensors come after the BS in the sequence as (35) guarantees. Similarly, (36) bounds the order of each node in the sequence by one more than the total number of transmitter nodes in the backbone. Finally, (37)–(45) are sign restrictions for the decision variables.

3.4. *The Node-Based MIP Model (NB-MIP) for Minimizing the Maximum Energy Consumption*

In this subsection, we introduce the Node-Based MIP model (NB-MIP) as an alternative to FB-MIP. The two models are different in several respects. FB-MIP is based on an arc-based disaggregation of the packet transmission, however, in the NB-MIP, we have node-based flow control. Moreover, FB-MIP traces the relay nodes from which each leaf node receives the transmission, whereas NB-MIP is concerned with whether all leaf nodes receive the transmission.

In Fig. 2, we present the optimal solutions for FB-MIP (in Fig. 2a) and NB-MIP (in Fig. 2b) for a WSN consisting of $|V| = 30$ nodes. Fig. 2a shows <u>all flows</u> that occur during packet transmission, while in Fig. 2b only flows between relay sensors are displayed. The representation in Fig. 2a is denser since the concern is on the path to each leaf node. However, Fig. 2b includes the paths to relay nodes. In NB-MIP, relay nodes are determined to ensure that all nodes in the WSN get the transmission from at least one of these relay nodes.

The sets, parameters, and some variables (e.g., $\mathcal{E}^{max}$, $\mathcal{E}_i$, $\mathcal{T}_{bsy,i}^b$, s_b, r_{il}^b, and x_{il}^b) are common in both FB-MIP and NB-MIP. Additional variables introduced for NB-MIP are listed in

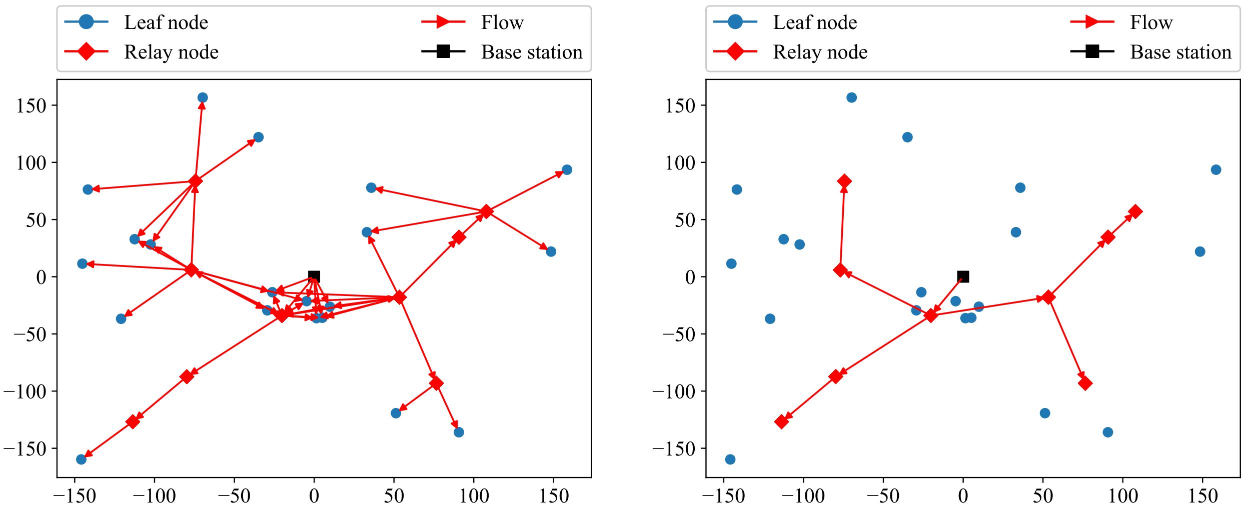

(a) FB-MIP

(b) NB-MIP

Figure 2: Optimal solutions of (a) FB-MIP and (b) NB-MIP for a network consisting of 30 nodes (i.e., $|V| = 30$).

Table 4: The list of additional variables used in NB-MIP.

Variables	
h^b_{ij}	the number of relay nodes, which receive broadcast packets from $i \in V$ via $j \in V$ in backbone-$b \in B$ (including j)
c^b_i	the total number of broadcast packets received by $i \in V$ in backbone-$b \in B$
y^b_i	1 if $i \in V$ receives broadcast packet in backbone-$b \in B$, 0 otherwise.

Table 4. In this model, we use c^b_i decision variables rather than m^b_{ij} to determine the aggregate flow incoming to each node $i \in V$. Similarly, variables, y^b_i, replace f^b_{ij} to keep track of the nodes in the backbone rather than the node pairs. Accordingly, g^b_{ij} variables do not exist in NB-MIP, either. Consequently, NB-MIP is defined in (46)–(67).

$$\text{Minimize} \quad \mathcal{E}^{max} \tag{46}$$

$$\text{s.t.} \quad \mathcal{T}^b_{bsy,i} = \mathcal{T}_{slot}\left(\sum_{l\in L} r^b_{il} + c^b_i\right), \qquad \forall i \in W, b \in B \tag{47}$$

$$\mathcal{E}_i = \sum_{b\in B}\sum_{l\in L} r^b_{il}\mathcal{E}^l_{tx} + \mathcal{E}_{rx}\sum_{b\in B} c^b_i + \mathcal{P}_{slp}\left(\sum_{b\in B} s_b\mathcal{T}_{rnd} - \sum_{b\in B}\mathcal{T}^b_{bsy,i}\right), \qquad \forall i \in W \tag{48}$$

$$y^b_i \le s_b, \qquad \forall i \in V, b \in B \tag{49}$$

$$My^b_i \ge s_b, \qquad \forall i \in V, b \in B \tag{50}$$

$$c^b_i \le My^b_i, \qquad \forall i \in V, b \in B \tag{51}$$

$$c^b_i \le s_b, \qquad \forall i \in V, b \in B \tag{52}$$

$$c^b_i \ge s_b - M(1 - y^b_i), \qquad \forall i \in V, b \in B \tag{53}$$

$$\sum_{l\in L} x^b_{il}a^j_{il} \le y^b_j, \qquad \forall i \in V, j \in V, b \in B \tag{54}$$

$$y^b_j \le \sum_{i\in V}\sum_{l\in L} x^b_{il}a^j_{il}, \qquad \forall j \in V, b \in B \tag{55}$$

$$\sum_{l\in L} x^b_{il} \le y^b_i, \qquad \forall i \in V, b \in B \tag{56}$$

$$h^b_{ij} \le M\sum_{l\in L} x^b_{il}a^j_{il}, \qquad \forall i \in V, j \in V, b \in B \tag{57}$$

$$h^b_{ii} = 0, \qquad \forall i \in V, b \in B \tag{58}$$

$$\sum_{i\in V} h^b_{iBS} = 0, \qquad \forall b \in B \tag{59}$$

$$\sum_{j\in V\setminus\{BS\}} h^b_{BS\,j} = \sum_{i\in V\setminus\{BS\}}\sum_{l\in L} x^b_{il}, \qquad \forall i \in V, b \in B \tag{60}$$

$$\sum_{j\in V} h^b_{ji} - \sum_{j\in V} h^b_{ij} = \sum_{l\in L} x^b_{il}, \qquad \forall i \in V\setminus\{BS\}, b \in B \tag{61}$$

$$\sum_{j\in V} h^b_{ij} \le |V|\sum_{l\in L} x^b_{il}, \qquad \forall i \in V, b \in B \tag{62}$$

$$\sum_{i\in V} h^b_{ij} \le |V|\sum_{l\in L} x^b_{jl}, \qquad \forall j \in V, b \in B \tag{63}$$

$$\sum_{i\in V} h^b_{ij} \ge \sum_{l\in L} x^b_{jl}, \qquad \forall j \in V\setminus\{BS\}, b \in B \tag{64}$$

$$(9), (11)-(16), (20)-(22), (26), (37), (39)-(42), (44)$$

$$c^b_i \ge 0, \qquad \forall b \in B, i \in V \tag{65}$$

$$h^b_{ij} \in \{0,1\}, \qquad \forall b \in B, i \in V, j \in V \tag{66}$$

$$y^b_i \in \{0,1\}, \qquad \forall b \in B, i \in V \tag{67}$$

Constraints (47) and (48) are analogous to (8) and (10) presented in FB-MIP. A similar analogy exists between (49) & (50) and (21) & (22). Constraints (51)–(53) guarantee that all sensors in a backbone $b \in B$ receive s_b packets, whereas (54)–(56) define the set of nodes in each backbone. The admissible transmissions are defined with (57)-(59). In NB-MIP, we eliminate the MTZ constraints. To this end, (60) and (61) are the flow constraints where each node in the backbone is assigned a unit of inflow. Consequently, (62)–(64) ensure that h^b_{ij} values are determined properly considering only the relay nodes in backbone $b \in B$. Finally, (65)–(67) are sign constraints for the new

Table 5: The list of additional variables defined for DA-NB-MIP.

Variables	
p_{ij}^b	1 if flow-(i, j) is used in backbone-$b \in B$ $\forall i, j \in V : i \neq j$, 0 otherwise
τ	delay in terms of hops
d_i	1 if $i \in V$ is the most energy-consuming node, 0 otherwise

variables.

3.5. Delay-Aware NB-MIP (DA-NB-MIP)

Both FB-MIP and NP-MIP aim to minimize the energy dissipation of the most energy-hungry node. In this subsection, we present the delay-aware counterpart of NB-MIP, which minimizes delay among all backbones. Indeed, minimizing the total number of hops within a backbone results in the minimization of the average broadcast delay for the whole network, therefore, we express delay in a backbone $b \in B$ in terms of the total number of hops in it. We establish the delay-aware model (i.e., DA-NB-MIP) based on the foundations provided by the NB-MIP model since it is more compact and scalable than FB-MIP. The additonal variables required for DA-NB-MIP are shown in Table 5 and the model is detailed in (68)–(76).

$$\text{Minimize} \quad \tau \tag{68}$$

$$\text{s.t.} \quad \tau \geq \sum_{(i,j)\in A} p_{ij}^b, \quad \forall b \in B \tag{69}$$

$$|V| p_{ij}^b \geq h_{ij}^b, \quad \forall i, j \in V, b \in B \tag{70}$$

$$h_{ij}^b \geq p_{ij}^b, \quad \forall i, j \in V, b \in B \tag{71}$$

$$\mathcal{E}^{max} \leq \mathcal{E}_i + M(1 - d_i), \quad \forall i \in V \tag{72}$$

$$\sum_{i\in V} d_i = 1 \tag{73}$$

$$(9), (11) - (16), (20) - (22), (26), (37),$$
$$(39) - (42),\ (44), (47) - (67)$$

$$p_{ij}^b \in \{0, 1\}, \quad \forall b \in B, i \in V, j \in V \tag{74}$$

$$\tau \geq 0 \tag{75}$$

$$d_i \in \{0, 1\}, \quad \forall i \in V \tag{76}$$

The objective function (68) minimizes delay (τ), which is related to the total number of hops in a broadcast backbone, over all backbones defined in (69). Constraints (70) and (71) ensure that p_{ij}^b is 1 when the flow-(i, j) is used in backbone $b \in B$. In addition to (12), we include (72) and (73) to calculate the amount of highest energy consumption among all nodes. Finally (74)–(76) are the sign restrictions for the new decision variables.

3.6. The Goal Programming (GP) Model

In this section, we define the GP model for WSN broadcasting supporting multiple backbones, which we utilize to analyze the tradeoff between minimizing delay and minimizing the maximum energy consumption. The mathematical expressions of these two conflicting objectives are

$$G_1 = \min \left\{ \max_{i\in V} \mathcal{E}_i \right\} = \min \mathcal{E}^{max}, \tag{77}$$

$$G_2 = \min \left\{ \max_{b\in B} \sum_{(i,j)\in A} p_{ij}^b \right\} = \min \tau. \tag{78}$$

The motivation of our GP model is to find a solution that minimizes the weighted maximum relative deviation from the optimal value of each objective. We denote the optimal values of the objectives G_1 and G_2 as G_1^* and G_2^*, respectively. Note that G_1^* is the optimal solution of NB-MIP defined in Section 3.4 and G_2^* is the optimal solution of DA-NB-MIP defined in Section 3.5. Consequently, the GP model is presented in (79)–(82)

$$\text{Minimize} \quad z \tag{79}$$

$$\text{s.t.} \quad (9), (11) - (16), (20) - (22), (26), (37),$$
$$(39) - (42),\ (44), (47) - (67), (69) - (76)$$

$$z \geq \gamma_i \frac{G_i - G_i^*}{G_i^*}, \quad \forall i \in \{1, 2\} \tag{80}$$

$$G_1 \geq G_1^* \tag{81}$$

$$G_2 \geq G_2^* \tag{82}$$

where γ_i is the weight associated with the relative deviation from the optimal value for each objective G_i, $\forall i \in \{1, 2\}$ to indicate its importance (i.e., $0 \leq \gamma_i \leq 1$, $\forall i \in \{1, 2\}$). For normalization, we make sure that $\gamma_1 + \gamma_2 = 1$. Moreover, z is the maximum weighted relative deviation value for the two objectives. The motivation of the GP model is to balance the tradeoff between G_1 and G_2 by minimizing z. For example, if $\gamma_1 = \gamma_2$, then G_1 and G_2 are equally important. If $\gamma_1 > \gamma_2$, then G_1 becomes more important than G_2, and vice versa. The steps of GP for a given topology and weight vector (γ_1, γ_2) are as shown in the flowchart in Fig. 3.

4. Analysis

In this section, we analyze the results of the optimal solutions of the MIP models, which are presented in Section 3, by exploring a fairly large parameter space. For statistical significance, the data points are obtained by averaging the results of 50 randomly generated instances. We use Python 3.8 to implement our models, which are solved with the CPLEX 20.1.0 solver on a computer with 64 GB of RAM, an Intel(R) Xeon(R) E7-4870 v2 @ 2.30 GHz CPU with 12 cores, and 100 GB of disk space.

In this study, we do not propose a new broadcasting algorithm for WSNs. Instead our main contribution is to characterize network lifetime for various operation strategies and parameter sets under optimal conditions (i.e., all our data points represent the maximum lifetime obtainable with the specified parameter and strategy configuration) without contaminating our results by incorporating implementation details that can lead to suboptimal behavior. By definition, there cannot be any algorithms which can surpass the optimal results we provide. As

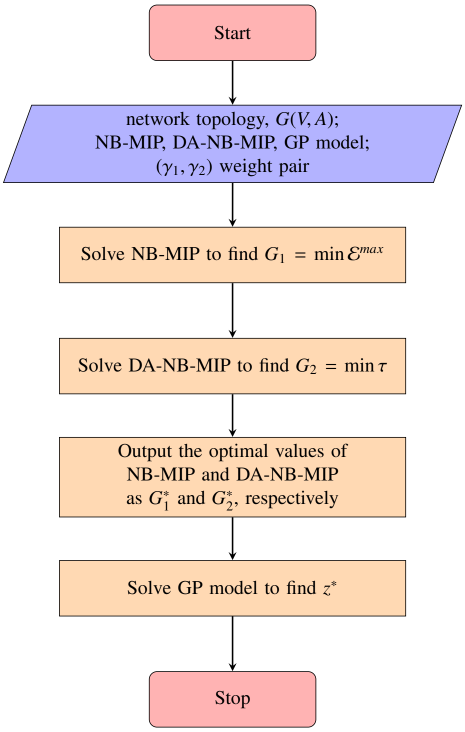

Figure 3: The Goal Programming flowchart.

such, providing comparisons with the suboptimal solution approaches proposed in the literature is not meaningful for characterizing network lifetime in WSN broadcasting under optimal conditions.

4.1. Solution Times for FB-MIP and NB-MIP

The solutions obtained with FB-MIP and NB-MIP are exactly the same for all problem instances we solved, which is important for functional verification of the optimization models. However, the most important difference between the models is that the solution times for FB-MIP and NB-MIP vary significantly. Given a solution time limit of three hours, the commercial solver (i.e., CPLEX) can solve FB-MIP to optimality only for the single backbone case (i.e., $N_b = 1$) where both FB-MIP and NB-MIP find the same optimal solutions. Besides, the average solution times (ASTs) for FB-MIP and NB-MIP are below 30 s and 1 s in all problem instances, respectively. Nevertheless, CPLEX can solve NB-MIP models to optimality for $2 \leq N_b \leq 6$ in reasonable solution times (i.e., ASTs of NP-MIP are less than 11 minutes in our scenarios), as shown in Table 6. Therefore, in the rest of the paper we opt to utilize the NB-MIP approach, which is shown to facilitate significantly lower solution times in comparison to the FB-MIP approach.

Table 6: ASTs of NB-MIP for $|V| = 60$.

N_b	2	3	4	5	6
AST (in s)	20	47	85	152	613

4.2. Minimization of Maximum Energy Consumption versus Total Energy Consumption

In this subsection, we present a comparative evaluation of the optimal solutions of two energy minimization approaches, which are both based on the NB-MIP model. The first approach is, actually, the one elaborated in subsection 3.4, which minimizes the energy dissipation of the maximum energy-consuming node (i.e., NB^{max} model). The second approach is also based on the MIP model given in subsection 3.4, however, the objective is the minimization of the total energy consumption (i.e., NB^{sum} model). In other words, the objective of NB^{max} is to minimize $\mathcal{E}^{max} = \{\max_{i \in V} \mathcal{E}_i\}$, whereas, in NB^{sum}, $\mathcal{E}^{sum} = \sum_{i \in V} \mathcal{E}_i$ is minimized. The comparison is for the single backbone case (i.e., $N_b = 1$). We investigate how the optimal backbone for each model performs in terms of average $\mathcal{E}^{max}$ (i.e., $\overline{\mathcal{E}^{max}}$) and $\mathcal{E}^{sum}$ (i.e., $\overline{\mathcal{E}^{sum}}$) metrics. More specifically, in Fig. 4a, we show the comparison with respect to average maximum energy consumption values whereas Fig. 4b presents the comparison of total energy consumption.

$\overline{\mathcal{E}^{max}}$ values for both approaches are presented in Fig. 4a. $\overline{\mathcal{E}^{max}}$ values obtained for NB^{sum} is relatively insensitive to the variation of the number of nodes in network size (i.e., $\overline{\mathcal{E}^{max}}$ values vary within 16.99–17.25 J band) because minimization of $\mathcal{E}^{max}$ is not enforced in NB^{sum} approach. $\overline{\mathcal{E}^{max}}$ values obtained with NB^{max} are always lower than those of NB^{sum} for all $|V|$. For example, $\overline{\mathcal{E}^{max}}$ values with NB^{max} for $|V| = 30$ and $|V| = 70$ are 7.63% and 18.04% lower than those of NB^{sum}, respectively. On the average, $\overline{\mathcal{E}^{max}}$ with NB^{max} is, approximately, 12.93% less than $\overline{\mathcal{E}^{max}}$ with NB^{sum}. $\overline{\mathcal{E}^{max}}$ obtained with NB^{max} decreases monotonically with increasing $|V|$ (i.e., $\overline{\mathcal{E}^{max}}$ decreases from 15.92 J to 14.08 J as $|V|$ increases from 30 to 70) because with increasing $|V|$ the network has more options to balance energy dissipation. Fig. 4b reveals that $\overline{\mathcal{E}^{sum}}$ values for both NB^{max} and NB^{sum} increase monotonically with increasing $|V|$ because total energy dissipation increases with the number of nodes in the network. Furthermore, $\overline{\mathcal{E}^{sum}}$ values of NB^{sum} are, on the average, approximately 23.05% lower than those of NB^{max}. It is natural that each model yields superior solutions according to the metric it optimizes (i.e., lower $\mathcal{E}^{max}$ with NB^{max} and lower $\mathcal{E}^{sum}$ with NB^{sum}). Nevertheless, our results confirm that minimizing the aggregate energy dissipation of the nodes does not, necessarily, lead to the minimization of the energy dissipation of the highest energy-consuming node.

Fig. 5 illustrates sample optimal backbones obtained with NB^{max} (Fig. 5a) and NB^{sum} (Fig. 5b) for a 30-node network. Each broadcast backbone is a tree rooted at the BS and contains all relay nodes through which all sensor nodes receive broadcast packets. The number of relay nodes is higher in Fig. 5a than the number of relay nodes in Fig. 5b. The reason behind this behavior is that balancing the energy dissipation among the nodes for reducing the energy dissipation of the highest energy-consuming node, which in turn results in higher network lifetime, requires more sensor nodes to become relay nodes in comparison to the aggregate energy minimization case.

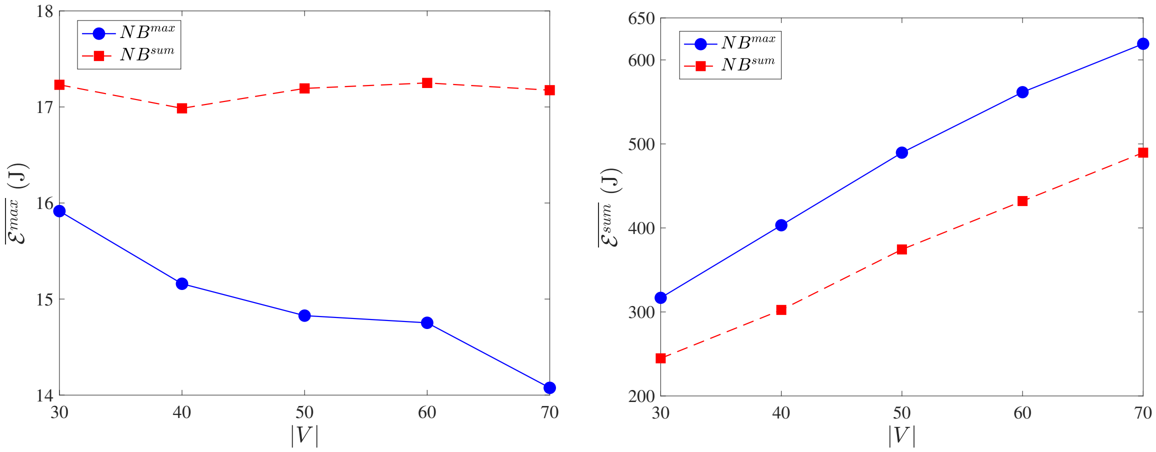

(a) $\overline{\mathcal{E}^{max}}$ vs. $|V|$ (b) $\overline{\mathcal{E}^{sum}}$ vs. $|V|$

Figure 4: Comparison of two average energy consumption objective values obtained from NB^{max} and NB^{sum} models for different values of $|V|$.

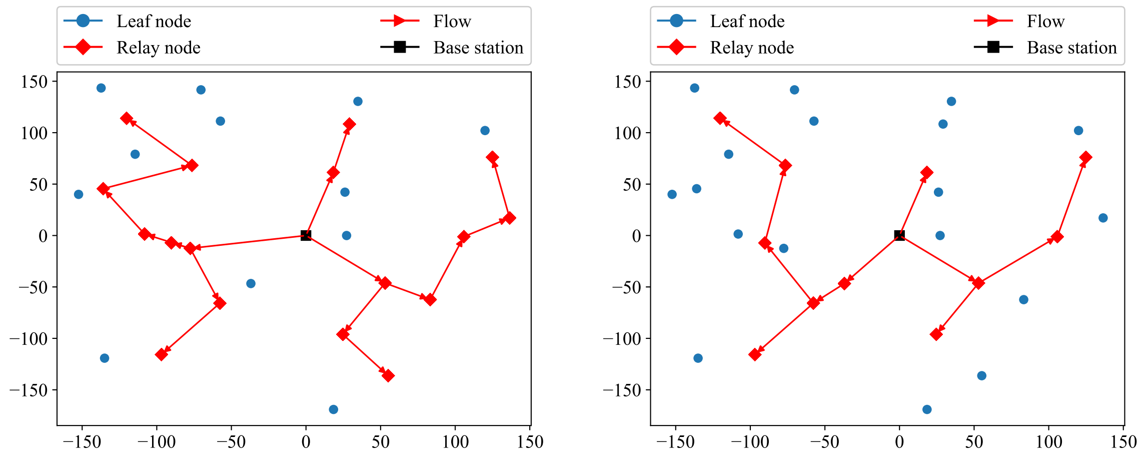

(a) NB^{max} (b) NB^{sum}

Figure 5: Backbones obtained with the optimal solutions of NB^{max} and NB^{sum} models in a 30-node sample network topology.

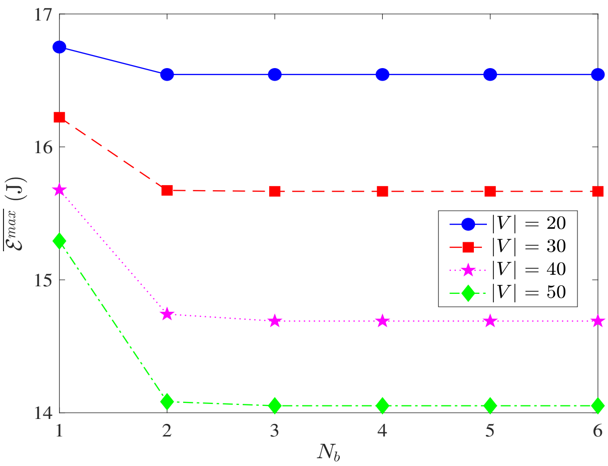

Figure 6: $\overline{\mathcal{E}^{max}}$ as a function of N_b with four $|V|$ values.

4.3. The Impact of the Number of Backbones

In this subsection, we explore the impact of utilizing multiple backbones on the MinMax energy optimization objective (i.e., $\mathcal{E}^{max}$) using the optimal solutions of the NB-MIP model. Fig. 6 presents $\overline{\mathcal{E}^{max}}$ as a function of N_b for $|V| \in \{20, 30, 40, 50\}$.

For constant N_b, $\overline{\mathcal{E}^{max}}$ values decrease as $|V|$ increases (e.g., for $N_b = 4$, $\overline{\mathcal{E}^{max}}$ =16.54 J, 15.66 J, 14.68 J, and 14.05 J for $|V| = 20, 30, 40$, and 50, respectively) because higher node densities facilitate better opportunities for load balancing among the sensor nodes. As a general trend, $\overline{\mathcal{E}^{max}}$ decreases as N_b increases (e.g., for $|V| = 50$, $\overline{\mathcal{E}^{max}}$ =15.29 J, 14.08 J, and 14.05 J for $N_b = 1, 2$, and 3, respectively) because the burden of relaying can be shared by a larger set of nodes with the availability of more broadcast backbones. However, the only significant decrease in $\overline{\mathcal{E}^{max}}$ occurs when N_b is increased from one to two (e.g., $\overline{\mathcal{E}^{max}}$ decreases by 1.25%, 3.39%, 5.99%, and 7.91% for $|V| = 20, 30, 40$, and 50, respectively). The decrease in $\overline{\mathcal{E}^{max}}$ when N_b is increased from two to three is insignificant (e.g., the

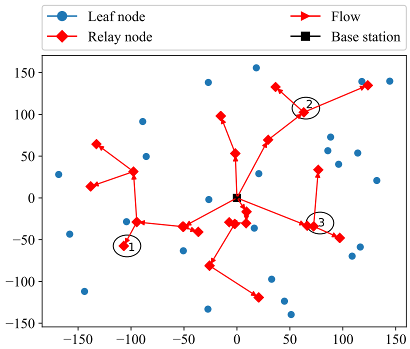

(a) $N_b = 1$: single backbone, $s_1 = 1440$

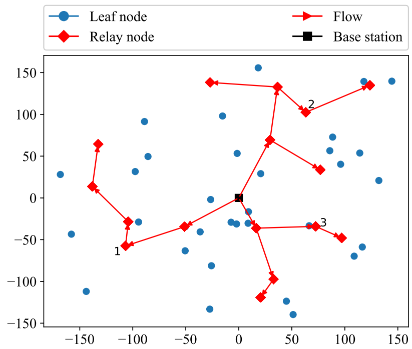

(b) $N_b = 2$: 1st backbone, $s_1 = 733$

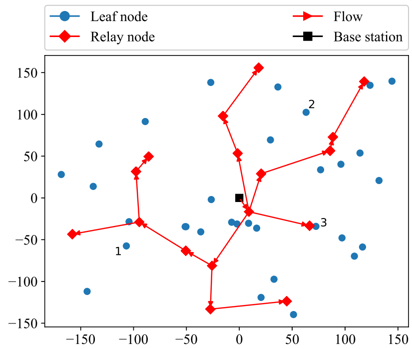

(c) $N_b = 2$: 2nd backbone, $s_2 = 707$

Figure 7: Backbones obtained with the optimal solutions of the MinMax energy objective in a 50-node sample network topology.

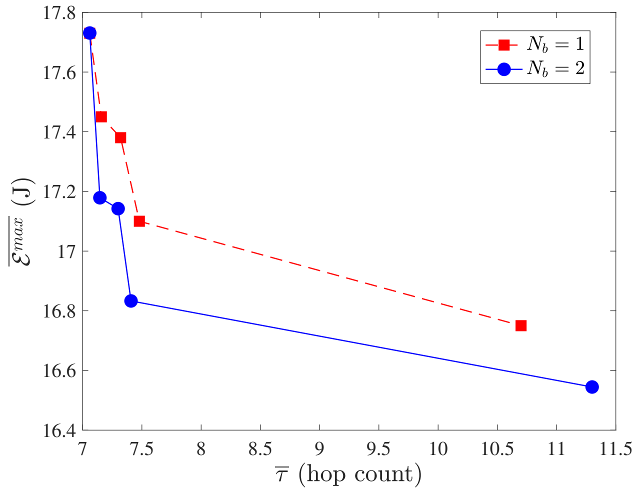

(a) |V| = 20

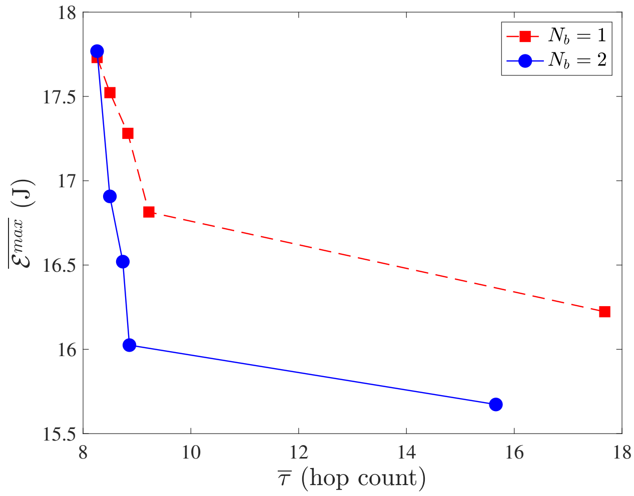

(b) |V| = 30

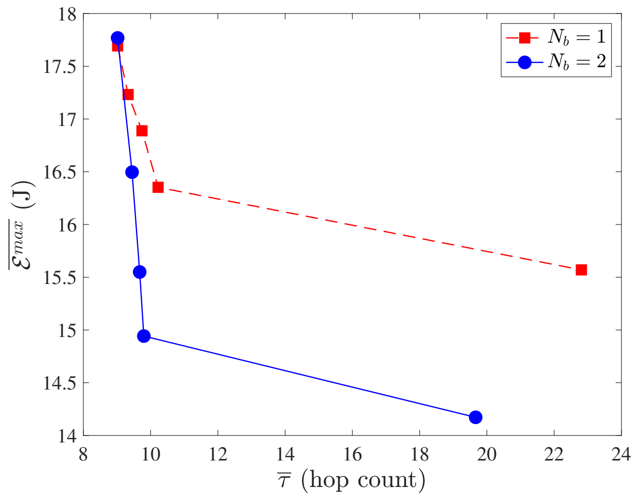

(c) |V| = 40

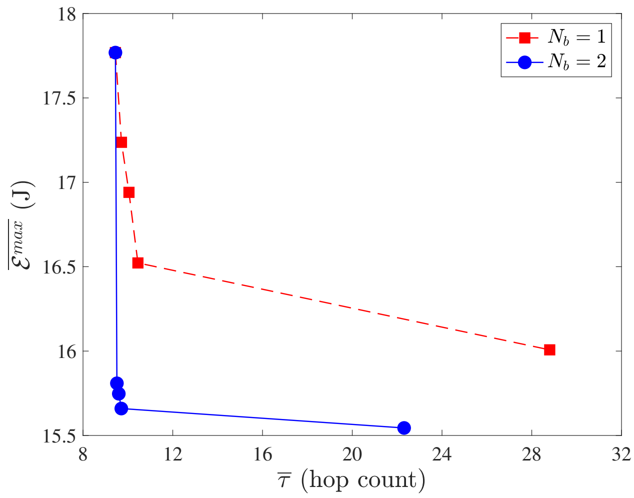

(d) |V| = 50

Figure 8: Energy vs. delay tradeoff with (a) |V| = 20, (b) |V| = 30, (c) |V| = 40, and (d) |V| = 50.

decrease in $\overline{\mathcal{E}^{max}}$ is, at most, 0.35%, for all cases). Increasing N_b beyond three does not result in any reduction in $\overline{\mathcal{E}^{max}}$. Indeed, the relation between $\overline{\mathcal{E}^{max}}$ and N_b is a typical case of the concept of diminishing marginal utilities. Nevertheless, $N_b = 2$ is sufficient to achieve the optimal or, at least, near-optimal $\overline{\mathcal{E}^{max}}$ values in broadcasting.

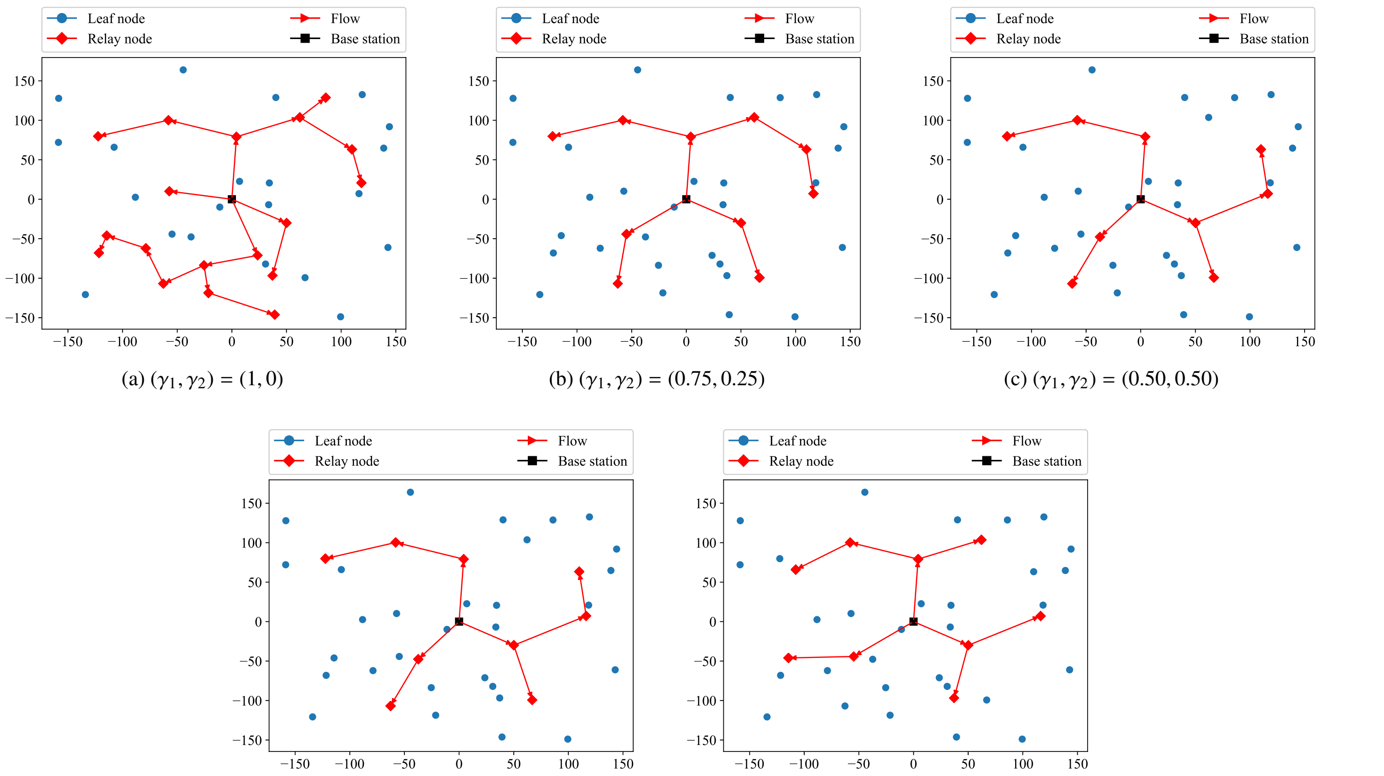

(a) $(\gamma_1, \gamma_2) = (1, 0)$

(b) $(\gamma_1, \gamma_2) = (0.75, 0.25)$

(c) $(\gamma_1, \gamma_2) = (0.50, 0.50)$

(d) $(\gamma_1, \gamma_2) = (0.25, 0.75)$

(e) $(\gamma_1, \gamma_2) = (0, 1)$

Figure 9: Backbones obtained with the optimal solutions of the GP model with a 40-node network topology.

To better illustrate the energy dissipation characteristics of broadcasting with $N_b = 1$ and $N_b = 2$, we present Fig. 7, where s_i denotes the number of broadcast packets transmitted on the backbone-i. $N_b = 1$ for Fig. 7a and $N_b = 2$ for Figs. 7b and 7c. For all N_b values, the BS transmits $M = 1440$ broadcast packets during an operational time of 24 hours in total (a single packet is generated at each round of duration 60 s). All sensor nodes receive all broadcast packets, yet only the relay nodes consume energy for broadcast packet transmissions. For the single backbone case depicted in Fig. 7a, all relay nodes participate in the transmission of all 1440 broadcast packets from the BS. The hotspot nodes (i.e., the nodes which consume the highest amount of energy) are node-1, node-2, and node-3, which are marked with circles. Energy consumption of these nodes is obtained as 14.59 J (i.e., $\mathcal{E}_1 = \mathcal{E}_2 = \mathcal{E}_3 = 14.59$ J). However, when $N_b = 2$, aforementioned hotspot nodes transmit only 733 broadcast packets since they are relay nodes only in the first backbone (Fig. 7b) but not in the second one (Fig. 7c). In this case, $\mathcal{E}_1 = 9.39$ J and $\mathcal{E}_2 = \mathcal{E}_3 = 10.32$ J. Hence, the total energy consumption of node-1, node-2, and node-3 reduce by 35.64%, 29.26%, and 29.26%, respectively, as N_b increases from 1 to 2. Hence, by allowing multiple backbones in broadcasting, we can mitigate the overburdening of nodes acting as broadcast relays.

4.4. Energy minimization vs. Delay Minimization Tradeoff

In this subsection, we analyze the tradeoff between minimizing $\mathcal{E}^{max}$ (energy dissipation of the highest energy-consuming node) and minimizing τ (delay, which is represented by the aggregate broadcast backbone size in terms of hops) objectives, which are integrated via the GP model presented in Section 3.6. Since $N_b \geq 3$ does not provide any significant reduction in $\mathcal{E}^{max}$, we set $N_b \in \{1, 2\}$. We choose $|V| \in \{20, 30, 40, 50\}$. The weights associated with goals G_1 (i.e., $\mathcal{E}^{max}$ minimization) and G_2 (i.e., τ minimization) are denoted by γ_1 and γ_2, respectively. We utilize five pairs of (γ_1, γ_2) values, which are $(0, 1), (0.25, 0.75), (0.50, 0.50), (0.75, 0.25)$, and $(1, 0)$.

Fig. 8 presents the Pareto front curves of the two conflicting objectives of $\mathcal{E}^{max}$ (y-axes) and τ (x-axes) for $|V| = 20$ (Fig. 8a), $|V| = 30$ (Fig. 8b), $|V| = 40$ (Fig. 8c), and $|V| = 50$ (Fig. 8d). In each sub-figure, Pareto frontiers are provided for both $N_b = 1$ and $N_b = 2$. The leftmost data point in each sub-figure corresponds to the case of $(\gamma_1, \gamma_2) = (0, 1)$, where minimization of τ has the utmost importance. On the other hand, the rightmost data point in each sub-figure has $(\gamma_1, \gamma_2) = (1, 0)$, where minimization of $\mathcal{E}^{max}$ has the highest importance. As we move from left to right along the x-axis, γ_1 values increase by 0.25 and γ_2 values decrease by 0.25. For example, in Fig. 8a, for $(\gamma_1, \gamma_2) = (0, 1)$ and $N_b = 1$, the average delay is 7.06 (i.e., $\overline{\tau} = 7.06$), and $\overline{\mathcal{E}^{max}} = 17.73$ J, whereas, for $(\gamma_1, \gamma_2) = (1, 0)$ and $N_b = 1$, $\overline{\tau} = 10.70$, and $\overline{\mathcal{E}^{max}} = 16.75$ J.

As the weight of $\mathcal{E}^{max}$ decreases from $\gamma_1 = 1$ to $\gamma_1 = 0$, its value increases by 5.85% with $N_b = 1$ and 7.17% with $N_b = 2$ for $|V| = 20$, 9.29% with $N_b = 1$ and 13.37% with $N_b = 2$ for $|V| = 30$, 13.64% with $N_b = 1$ and 25.38% with $N_b = 2$ for

$|V| = 40$, and 11.00% with $N_b = 1$ and 14.31% with $N_b = 2$ for $|V| = 50$. The variation in τ is higher with change in its weight in comparison to $\mathcal{E}^{max}$. As the weight of τ decreases from $\gamma_2 = 1$ to $\gamma_2 = 0$, its value increases by 51.56% with $N_b = 1$ and 60.06% with $N_b = 2$ for $|V| = 20$, 114.04% with $N_b = 1$ and 89.59% with $N_b = 2$ for $|V| = 30$, 152.88% with $N_b = 1$ and 118.03% with $N_b = 2$ for $|V| = 40$, and 204.94% with $N_b = 1$ and 136.24% with $N_b = 2$ for $|V| = 50$. Therefore, zeroing the weight of any objective leads to significant deterioration in the other one, which is especially destructive for τ. As the number of nodes increases, vulnerability of the delay objective also increases because to minimize $\mathcal{E}^{max}$ higher number of nodes are included in the backbone, which inflates the delay significantly.

Prioritization of the WSN operation characteristics depends on application specific requirements, which can be tuned by utilizing proper weights (i.e., γ_1 and γ_2). The equal priority operating point (i.e., $\gamma_1 = \gamma_2 = 0.5$) facilitates a fair balance for both objectives for all $|V|$ values (i.e., neither of the objectives deteriorate significantly when compared to their highest priority operating points). For example, the percentage increase in $\overline{\tau}/\overline{\mathcal{E}^{max}}$ values with $\gamma_1 = \gamma_2 = 0.5$ and $N_b = 1$ in comparison to the corresponding highest priority cases, i.e., $(\gamma_1, \gamma_2) = (1, 0)$ for $\mathcal{E}^{max}$ and $(\gamma_1, \gamma_2) = (0, 1)$ for τ, are 3.69%/4.18% for $|V| = 20$, 6.91%/8.01% for $|V| = 30$, 8.03%/10.68% for $|V| = 40$, and 6.39%/7.68% for $|V| = 50$.

As a general trend in Fig. 8 for all node densities, utilization of multiple backbones (i.e., $N_b = 2$) results in lower $\overline{\mathcal{E}^{max}}$ and $\overline{\tau}$ values in comparison to the single backbone case ($N_b = 1$). For example, with $(\gamma_1, \gamma_2) = (0.75, 0.25)$ the percentage decrease obtained in $\overline{\tau}/\overline{\mathcal{E}^{max}}$ values with $N_b = 2$ with respect to the values obtained with $N_b = 1$ are 0.94%/1.56% for $|V| = 20$, 3.91%/4.70% for $|V| = 30$, and 4.15%/8.62% for $|V| = 40$. In fact, our results reveal that the flexibility of employing multiple backbones is necessary for improving both of the optimization objectives (delay and energy) in comparison to the single backbone case.

Fig. 9 illustrates broadcast backbones, obtained by the optimal solutions of the GP model, on a sample network topology consisting of 40 nodes. More specifically, Figs. 9a, 9b, 9c, 9d, and 9e are obtained with (γ_1, γ_2) values of $(1, 0)$, $(0.75, 0.25)$, $(0.50, 0.50)$, $(0.25, 0.75)$, and $(0, 1)$, respectively. For the ease of exposition, we provide the single backbone case (i.e., $N_b = 1$) in all sub-figures. $\tau/\mathcal{E}^{max}$ values in Figs. 9a, 9b, 9c, 9d, and 9e are 18/14.91 J, 10/14.91 J, 9/15.88 J, 9/15.88 J, and 9/17.77 J, respectively. As γ_1 decreases from one to zero and γ_2 increases from zero to one, $\mathcal{E}^{max}$ increases by 19.16% and τ decreases by 50.00%. Maximum delay (in terms of the length of the longest BS-to-relay hop distance) also decreases in parallel with our delay metric from 6 (Fig. 9a) to 3 (Fig. 9e), which corresponds to a 50.00% reduction. It is possible to maintain the lowest $\mathcal{E}^{max}$ value (14.91 J) while achieving a reasonably low τ value (10) by choosing $(\gamma_1, \gamma_2) = (0.75, 0.25)$ in this scenario. On the other hand, it is also possible to maintain the lowest τ value (9) while mildly sacrificing from the $\mathcal{E}^{max}$ value (15.88 J) by choosing $(\gamma_1, \gamma_2) = (0.5, 0.5)$.

5. Conclusion

Network lifetime is, arguably, the most crucial performance metric for WSNs [11, 12, 43, 44, 45]. In this study, we investigate energy dissipation and delay characteristics of broadcasting in WSNs. Utilizing multiple backbones facilitates energy dissipation balancing in broadcasting, which is a research problem that has never been investigated systematically within a mathematical programming-based optimization framework. Minimizing delay is also essential for the timely distribution of control/coordination information to the whole network, yet energy minimization and delay minimization are conflicting goals. We create a goal programming-based optimization framework to analyze the tradeoffs between energy minimization and delay minimization for broadcasting in WSNs with multiple backbones. Our novel optimization framework enables us to perform comprehensive and holistic characterization of energy dissipation and delay aspects of broadcasting in WSNs under ideal yet realistic operating conditions. We explore a wide parameter space through the optimal solutions of our models, which outline the boundaries of achievable performance bounds. The main novel contributions of this study are enumerated as follows:

1. We construct two alternative optimization models for the minimization of the energy dissipation of the maximum energy-consuming node supporting multiple backbones in WSN broadcasting, which are the node-based model (NB-MIP) and the flow-based model (FB-MIP). Optimal solutions of both models give exactly the same results, which is invaluable for verification. However, the solution times of the node-based model are, at least, an order of magnitude lower than those of the flow-based model.
2. We performed a comparative analysis of minimizing the aggregate energy dissipation and minimizing the energy dissipation of the highest energy-consuming node for WSN broadcasting to determine the energy balancing aspects of each approach, which reveals that the latter approach results in up to more than 9% lower maximum energy dissipation than the former approach.
3. Our results show that utilizing multiple backbones reduces the maximum energy dissipation significantly (i.e., more than 8%) when compared to the single backbone case. However, employing more than two backbones does not result in any significant decrease in maximum energy dissipation beyond that can be achieved by two backbones.
4. GP-based joint optimization of energy dissipation and delay with multiple backbones results in more than 8% reduction in maximum energy dissipation in comparison to the single backbone case without sacrificing the delay performance, likewise, delay can be reduced by more than 20% without deteriorating the energy dissipation.
5. It is also possible to improve both delay and energy dissipation characteristics significantly with multiple backbones in comparison to the single backbone case by assigning proper priorities to both delay and energy dissipa-

tion objectives via GP. Actually, delay and energy dissipation values with two backbones are more than 4% and 7% lower than those obtained with the single backbone case, respectively, when both objectives are assigned the same weights to facilitate equal priorities.

There are various future research avenues to be explored based on the results of our study, which can be enumerated as follows:

1. We build an exact optimization model and resort to commercial solvers to obtain optimal results. However, our model cannot be solved to optimality for extremely large problem instances. Therefore, it is necessary to develop efficient solution approaches to be able to solve larger problem instances.
2. Design and analysis of distributed broadcast algorithms supporting multiple backbones for concurrently minimizing delay and maximizing network lifetime in WSNs is a promising research problem.
3. Investigation of the tradeoff between network lifetime, delay, and the number of backbones for broadcasting in WSNs by utilizing experimental testbeds is also an important research topic.

References

[1] J. Yick, B. Mukherjee, D. Ghosal, Wireless sensor network survey, Comput. Netw. 52 (12) (2008) 2292–2330.

[2] J. T. Correll, J. T. McNaughton, Igloo white, Air Force Mag. 87 (11) (2004) 56–61.

[3] D. Kandris, C. Nakas, D. Vomvas, G. Koulouras, Applications of wireless sensor networks: an up-to-date survey, Appl. Syst. Inno. 3 (1) (2020) 14.

[4] C. N. Ferdous, L. Karimi, D. R. Gaur, Integer programs for contention aware connected dominating sets in wireless multi-hop networks, in: Proc. IEEE Wirel. Commun. Netw. Conf. (WCNC), 2022, pp. 2142–2147.

[5] M. X. Cheng, J. Sun, M. Min, D.-Z. Du, Energy-efficient broadcast and multicast routing in ad hoc wireless networks, in: Proc. IEEE Int. Perform. Comput. Commun. Conf. (PCCC), 2003, pp. 87–94.

[6] L. Cheng, J. Niu, C. Luo, L. Shu, L. Kong, Z. Zhao, Y. Gu, Towards minimum-delay and energy-efficient flooding in low-duty-cycle wireless sensor networks, Comput. Netw. 134 (2018) 66–77.

[7] M. Rajeswari, K. Thirugnanasambandam, R. Raghav, U. Prabu, D. Saravanan, D. K. Anguraj, Flower pollination algorithm with powell's method for the minimum energy broadcast problem in wireless sensor network, Wireless Pers. Commun. 119 (2021) 1111–1135.

[8] M. Čagalj, J.-P. Hubaux, C. Enz, Minimum-energy broadcast in all-wireless networks: NP-completeness and distribution issues, in: Proc. Int. Conf. Mobile Comput. Netw. (MobiCom), 2002, pp. 172–182.

[9] J. E. Wieselthier, G. D. Nguyen, A. Ephremides, On the construction of energy-efficient broadcast and multicast trees in wireless networks, in: Proc. IEEE Conf. Comput. Commun. (INFOCOM), Vol. 2, 2000, pp. 585–594.

[10] H. Hernández, C. Blum, Minimum energy broadcasting in wireless sensor networks: An ant colony optimization approach for a realistic antenna model, Appl. Soft Comput. 11 (8) (2011) 5684–5694.

[11] H. U. Yildiz, B. Tavli, H. Yanikomeroglu, Transmission power control for link-level handshaking in wireless sensor networks, IEEE Sens. J. 16 (2) (2015) 561–576.

[12] S. Kurt, H. U. Yildiz, M. Yigit, B. Tavli, V. C. Gungor, Packet size optimization in wireless sensor networks for smart grid applications, IEEE Trans. Ind. Electron. 64 (3) (2017) 2392–2401.

[13] I. Kang, R. Poovendran, Maximizing static network lifetime of wireless broadcast ad hoc networks, in: Proc. IEEE Int. Conf. Commun. (ICC), Vol. 3, 2003, pp. 2256–2261.

[14] S. Xiao, L. Pan, J. Liu, B. Li, X. Yuan, Distributed broadcast with minimum latency in asynchronous wireless sensor networks under SINR-based interference, Int. J. Distrib. Sens. N. 9 (11) (2013) 506797.

[15] T. Shu, W. Liu, T. Wang, Q. Deng, M. Zhao, N. N. Xiong, X. Li, A. Liu, Broadcast based code dissemination scheme for duty cycle based wireless sensor networks, IEEE Access 7 (2019) 105258–105286.

[16] S. Wu, J. Niu, W. Chou, M. Guizani, Delay-aware energy optimization for flooding in duty-cycled wireless sensor networks, IEEE T. Wirel. Commun. 15 (12) (2016) 8449–8462.

[17] K. Breschi, J. Bernard, Construction of a minimum energy broadcast backbone with bounded delay in heterogeneous wireless sensor networks, in: Proc. IEEE Symp. Comput. Commun. (ISCC), 2017, pp. 1306–1311.

[18] J. Vales-Alonso, E. Egea-López, A. Martínez-Sala, P. Pavon-Marino, M. V. Bueno-Delgado, J. García-Haro, Performance evaluation of MAC transmission power control in wireless sensor networks, Comput. Netw. 51 (6) (2007) 1483–1498.

[19] J. E. Wieselthier, G. D. Nguyen, A. Ephremides, Algorithms for energy-efficient multicasting in static ad hoc wireless networks, Mobile Netw. Appl. 6 (3) (2001) 251–263.

[20] O. Egecioglu, T. Gonzalez, Minimum-energy broadcast in simple graphs with limited node power, in: Proc. IASTED Int. Conf. Parall. Distr. Comput. Syst. (PDCS), 2001, pp. 334–338.

[21] J. Cartigny, D. Simplot, I. Stojmenovic, Localized minimum-energy broadcasting in ad-hoc networks, in: Proc. IEEE Conf. Comput. Commun. (INFOCOM), Vol. 3, 2003, pp. 2210–2217.

[22] R. Montemanni, P. Mahdabi, A linear programming-based evolutionary algorithm for the minimum power broadcast problem in wireless sensor networks, J. Math. Model. Algo. 10 (2) (2011) 145–162.

[23] Z. Cao, X. Zheng, Q. Ma, X. Miao, COFlood: Concurrent opportunistic flooding in asynchronous duty cycle networks, in: Proc. IEEE Int. Conf. Sens. Commun. Netw. (SECON), 2021, pp. 1–9.

[24] A. K. Das, R. J. Marks, M. El-Sharkawi, P. Arabshahi, A. Gray, Minimum power broadcast trees for wireless networks: integer programming formulations, in: Proc. IEEE Conf. Comput. Commun. (INFOCOM), Vol. 2, 2003, pp. 1001–1010.

[25] W. Zhang, J. Liang, X. Liang, On the computation of virtual backbones with fault tolerance in heterogeneous wireless sensor networks, IEEE T. Mobile Comput. 21 (8) (2022) 2922–2938.

[26] A. K. Das, R. J. Marks, M. El-Sharkawi, P. Arabshahi, A. Gray, MDLT: a polynomial time optimal algorithm for maximization of time-to-first-failure in energy constrained wireless broadcast networks, in: Proc. IEEE Glob. Telecommun. Conf. (GLOBECOM), Vol. 1, 2003, pp. 362–366.

[27] N. Papanna, A. R. M. Reddy, M. Seetha, Eelam: Energy efficient lifetime aware multicast route selection for mobile ad hoc networks, Appl. Comput. and Inform. 15 (2) (2019) 120–128.

[28] G. Deng, S. K. S. Gupta, WSN19-1: Maximizing broadcast tree lifetime in wireless ad hoc networks, in: Proc. IEEE Glob. Telecommun. Conf. (GLOBECOM), 2006, pp. 1–5.

[29] R. Montemanni, Maximum lifetime broadcasting topologies in wireless sensor networks: advanced mathematical programming models, in: Proc. Hawaii Int. Conf. Syst. Sci. (HICSS), 2009, pp. 1–10.

[30] R. Montemanni, et al., Integer programming formulations for maximum lifetime broadcasting problems in wireless sensor networks, Wirel. Sens. Netw. 2 (12) (2010) 924.

[31] W. Yanbin, W. Zhuofei, Z. Jing, L. Zhijuan, M. Xiaomin, Analysis and adaptive optimization of vehicular safety message communications at intersections, Ad Hoc Netw. 107 (2020) 102241.

[32] Q. Chen, Z. Cai, L. Cheng, H. Gao, J. Li, Structure-free broadcast scheduling for duty-cycled multihop wireless sensor networks, IEEE T. Mobile Comput. 21 (12) (2022) 4624–4641.

[33] A. A. Lata, M. Kang, A review on broadcasting protocols for duty-cycled wireless sensor networks, in: Proc. Int. Conf. Ubiq. Future Netw. (ICUFN), 2019, pp. 649–652.

[34] M. Laumanns, L. Thiele, E. Zitzler, An efficient, adaptive parameter variation scheme for metaheuristics based on the epsilon-constraint method, Eur. J. Oper. Res. 169 (3) (2006) 932–942.

[35] M. A. Ramos, M. Boix, L. Montastruc, S. Domenech, Multiobjective optimization using goal programming for industrial water network design, Ind. Eng. Chem. Res. 53 (45) (2014) 17722–17735.

[36] B. Aouni, O. Kettan, Goal programming model: A glorious history and a promising future, Eur. J. Oper. Res. 133 (2001) 225–231.

[37] Z. Fei, B. Li, S. Yang, C. Xing, H. Chen, L. Hanzo, A survey of multi-objective optimization in wireless sensor networks: Metrics, algorithms, and open problems, IEEE Commun. Surveys Tuts. 19 (1) (2016) 550–586.
[38] C. A. De Kluyver, An exploration of various goal programming formulations – with application to advertising media scheduling, J. Oper. Res. Soc. 30 (2) (1979) 167–171.
[39] C. Romero, Multi-objective and goal-programming approaches as a distance function model, J. Oper. Res. Soc. 36 (3) (1985) 249–251.
[40] M. Zeleny, The pros and cons of goal programming, Comput. Oper. Res. 8 (4) (1981) 357–359.
[41] K. Mumtaz, A multi-objective bi-level location problem for heterogeneous sensor networks with hub-spoke topology, Comput. Netw. 181 (2020) 107551.
[42] A.-J. Garcia-Sanchez, F. Garcia-Sanchez, D. Rodenas-Herraiz, J. Garcia-Haro, On the optimization of wireless multimedia sensor networks: A goal programming approach, Sensors 12 (9) (2012) 12634–12660.
[43] V. Arora, V. Sharma, M. Sachdeva, ACO optimized self-organized tree-based energy balance algorithm for wireless sensor network, J. Ambient Intell. Human. Comput. 10 (2019) 4963–4975.
[44] P. K. Poonguzhali, N. P. Ananthamoorthy, Improved energy efficient WSN using ACO based HSA for optimal cluster head selection, Peer-to-Peer Netw. Appl. 13 (2020) 1102–1108.
[45] V. K. Arora, V. Sharma, A novel energy-efficient balanced multi-hop routing scheme (EBMRS) for wireless sensor networks, Peer-to-Peer Netw. Appl. 14 (2021) 807–820.